The rate of DNA evolution: Effects of body size and temperature on the molecular clock

James F. Gillooly*†, Andrew P. Allen*, Geoffrey B. West‡§, and James H. Brown*‡

*Department of Biology, University of New Mexico, Albuquerque, NM 87131; ‡Santa Fe Institute, 1399 Hyde Park Road, Santa Fe, NM 87501; and §Theoretical Physics Division, Los Alamos National Laboratory, MS B285, Los Alamos, NM 87545

Communicated by Murray Gell-Mann, Santa Fe Institute, Santa Fe, NM, November 9, 2004 (received for review March 26, 2004)

Observations that rates of molecular evolution vary widely within and among lineages have cast doubts on the existence of a single "molecular clock." Differences in the timing of evolutionary events estimated from genetic and fossil evidence have raised further questions about the accuracy of molecular clocks. Here, we present a model of nucleotide substitution that combines theory on metabolic rate with the now-classic neutral theory of molecular evolution. The model quantitatively predicts rate heterogeneity and may reconcile differences in molecular- and fossil-estimated dates of evolutionary events. Model predictions are supported by extensive data from mitochondrial and nuclear genomes. By accounting for the effects of body size and temperature on metabolic rate, this model explains heterogeneity in rates of nucleotide substitution in different genes, taxa, and thermal environments. This model also suggests that there is indeed a single molecular clock, as originally proposed by Zuckerkandl and Pauling [Zuckerkandl, E. & Pauling, L. (1965) in *Evolving Genes and Proteins*, eds. Bryson, V. & Vogel, H. J. (Academic, New York), pp. 97–166], but that it "ticks" at a constant substitution rate per unit of mass-specific metabolic energy rather than per unit of time. This model therefore links energy flux and genetic change. More generally, the model suggests that body size and temperature combine to control the overall rate of evolution through their effects on metabolism.

mutation | metabolic theory | allometry | substitution

Completion of the modern evolutionary synthesis will require better understanding of the molecular processes of evolutionary change. The speed of molecular evolution can be measured as the rate of genetic divergence of descendants from a common ancestor, so the rate of molecular evolution can be quantified in terms of the changes in the nucleotide sequences that comprise the genome. Observations that rates of molecular evolution vary widely within and among lineages have raised doubts about the existence of a single "molecular clock," as originally proposed by Zuckerkandl and Pauling (1). The accuracy of molecular clocks is further called into question because molecular estimates of divergence time often disagree with the fossil record (2, 3). Understanding the factors responsible for rate heterogeneity is key to resolving differences between molecular and fossil-based estimates of important evolutionary events [e.g., Cambrian explosion (4, 5) and proliferation of modern mammalian orders (2)]. More generally, understanding rate heterogeneity may yield insight into the factors affecting overall rates of evolution.

Variations in rates of nucleotide substitution have been correlated with body size, metabolic rate (6), generation time (7), and environmental temperature (8, 9). Differences also have been observed between endotherms and ectotherms (6, 10). This rate heterogeneity most often is attributed to one of two causes, metabolic rate or generation time. According to the metabolic rate hypothesis, most mutations are caused by genetic damage from free radicals produced as byproducts of metabolism, so mutation rates should be related to cellular or mass-specific metabolic rates (6). According to the generation time hypothesis, most mutations are caused by errors in DNA replication during cell division, so mutation rates should be related to the number of divisions in germ cell lines and hence to generation times (7). Distinguishing between these hypotheses has been difficult because free radical production and generation time both vary with metabolic rate (6, 11), which in turn varies with body size and temperature (12).

Here, we propose a model that predicts heterogeneity in rates of molecular evolution by combining principles of allometry and biochemical kinetics with Kimura's neutral theory of evolution. The model quantifies the relationship between rates of energy flux and genetic change based explicitly on the effects of body size and temperature on metabolic rate. Although the model does not distinguish between the metabolic rate and generation time hypotheses, it accounts for much of the observed rate heterogeneity across a wide range of taxa in diverse environments. Recalibrating the molecular clocks by using metabolic rate reconciles some fossil- and molecular-based estimates of divergence.

The Model

Metabolic rate is the rate at which energy and materials are taken up from the environment and used for maintenance, growth, and reproduction. It ultimately governs most biological rate processes, including the two generally thought to control mutation rate: free radical production rate and generation time (6, 7, 12, 13). Metabolic rate likely affects other processes, such as DNA repair and environmentally induced mutagenesis, that influence rates of nucleotide substitution (6). Mass-specific metabolic rate (B) varies with body size, M, and temperature, T, as

$$B = b_o M^{-1/4} e^{-E/kT}, \quad [1]$$

where b_o is a coefficient independent of body size and temperature (12). The body size term, $M^{-1/4}$, has its origins in the fractal-like geometry of biological exchange surfaces and distribution networks (14). The Boltzmann or Arrhenius factor, $e^{-E/kT}$, underlies the temperature dependence of metabolic rate, where E is an average activation energy for the biochemical reactions of metabolism ($\approx$0.65 eV) (12), k is Boltzmann's constant (8.62×10^{-5} eV·K^{-1}), and T is absolute temperature in degrees Kelvin. Eq. **1** explains most of the variation in the metabolic rates of plants, animals, and microbes (12).

When combined with assumptions of the neutral theory (15), Eq. **1** also can be used to characterize rates of molecular evolution. The first assumption is that molecular evolution is caused primarily by neutral mutations that randomly drift to fixation in a population, resulting in nucleotide substitutions (15). This assumption is consistent with theory and data demonstrating that deleterious mutations have only a negligible chance of becoming fixed in a population because of purifying selection (16), and that favorable mutations occur very rarely

Abbreviation: My, millions of years.

†To whom correspondence should be addressed. E-mail: gillooly@unm.edu.

www.pnas.org/cgi/doi/10.1073/pnas.0407735101

(17). Under this assumption, the rate of nucleotide substitution per generation is equal to the neutral mutation rate per generation and is independent of population size (15). The second assumption is that point mutations, and therefore substitutions, occur at a rate proportional to B. This idea assumes that most mutations are caused by some combination of free radical damage, replication errors, and other processes that ultimately are consequences of metabolism. Together, these two assumptions imply that the nucleotide substitution rate, α, defined as the number of substitutions per site per unit time, varies with body size and temperature as

$$\alpha = f\nu B = f\nu b_o M^{-1/4} e^{-E/kT}, \qquad [2]$$

where f is the proportion of point mutations that are selectively neutral, and ν is the number of point mutations per site per unit of metabolic energy expended by a unit mass of tissue (g mutations site^{-1}·J^{-1}). Thus, the product $f\nu$ is the neutral mutation rate per unit of mass-specific metabolic energy and, following Kimura's neutral theory, the substitution rate (see *Appendix 1*, which is published as supporting information on the PNAS web site). If the body size and temperature dependence of substitution rate is controlled by B, then $f\nu$ is predicted to be a constant independent of M and T. Consequently, Eq. **2** predicts the existence of a molecular clock that "ticks" at a constant rate per unit of mass-specific metabolic energy flux rather than per unit of time. On average, a certain quantity of metabolic energy transformation within a given mass of tissue causes a substitution in a given gene regardless of body size, temperature, or taxon. Eq. **2** therefore predicts a 100,000-fold increase in substitution rates across the biological size range ($\approx 10^8$ g of whales to $\approx 10^{-12}$ g of microbes) and a 34-fold increase in substitution rates across the biological temperature range (≈0–40°C).

Rearranging terms in Eq. **2** and taking logarithms yields:

$$\ln(\alpha M^{1/4}) = -E\left(\frac{1}{kT}\right) + C \qquad [3]$$

or

$$\ln(\alpha e^{E/kT}) = -1/4 \ln M + C, \qquad [4]$$

where $C = \ln(f\nu b_o)$.

Model Predictions

Eqs. **3** and **4** correct for mass and temperature, respectively, and lead to three explicit predictions. The first prediction is that the logarithms of mass-corrected substitution rates should be linear functions of $1/kT$ with slopes of $-E \approx -0.65$ eV (Eq. **3**), reflecting the kinetics of aerobic metabolism. The second prediction is that the logarithms of temperature-corrected substitution rates should be linear functions of $\ln M$ with slopes of approximately $-1/4$ (Eq. **4**), reflecting the allometric scaling of mass-specific metabolic rate (14). Finally, if these first two predictions hold, then the third prediction is that, for a given gene, the number of substitutions per site per unit mass-specific metabolic energy, $f\nu$, should be approximately invariant across taxa.

Methods

Calculation of Substitution Rates. Estimated rates of substitution, α, were compiled from multiple published sources for mitochondrial and nuclear genomes (respectively, *Appendixes 2* and *3*, which are published as supporting information on the PNAS web site). Together, these data represent several major taxonomic groups (e.g., invertebrates, fish, amphibians, reptiles, birds, and mammals), which span 10 orders of magnitude in body size and the biological temperature range 0°C to 40°C. Sequence divergence, D, was estimated by using direct sequencing methods for all sequences considered here except for the entire mitochondrial genome, where the restriction fragment length polymorphism technique was used. For the mitochondrial genome, estimates of sequence divergence were from four different coding regions (12s rRNA, 16s RNA, cytochrome *b*, and whole genome). For the nuclear genome, estimates of sequence divergence were from two published sources based on rates of silent substitution in coding regions. In the first source, divergence estimates were calculated for 11 pairs of primates based on globin gene data (6). In the second source, estimates were obtained for 23 pairs of mammalian taxa that encompass 17,208 protein-coding DNA sequences from 5,669 nuclear genes and 326 species (18) (*Appendix 3*).

Times of divergence, τ in millions of years (My), were independently estimated by using paleontological data (e.g., fossil records and geological events), and varied by ≈2 orders of magnitude for the mitochondrial data (0.43–38 My) and 1 order of magnitude for the nuclear data (5.5–56.5 My) (*Appendixes 2* and *3*). Substitution rates were then calculated as $\alpha = D/2\tau$, which are the average for the two lineages over time τ (*Appendix 4*, which is published as supporting information on the PNAS web site). Although not all sources used the same mathematical model to estimate D in mitochondrial genomes, variation caused by differences in methodology is small (19) compared with the predicted effects of body size and temperature.

Body Size and Temperature Estimates. The formula for estimating substitution rate ($\alpha = D/2\tau$) is an average for two descendent lineages that may differ in body mass. To account for differences in substitution rates caused by differences in body mass between the two lineages, we take the "quarter-power average," which controls for the greater influence of the smaller, more rapidly evolving lineage on the calculated substitution rate (*Appendix 4*). Body temperatures of endothermic birds and mammals were estimated from the literature and varied between ≈35°C and 40°C. Body temperatures of ectotherms were estimated as the mean annual ambient temperature where the organisms presently occur, or in the case of some fishes, the temperature of the preferred habitat. This estimation assumes that extant ectotherms are approximately in thermal equilibrium with their environment, and that they occur in a similar thermal environment as their ancestors.

Assessing Effects of Body Mass and Temperature. Our methods for estimating body size and temperature likely introduce substantial error into these predictor variables. This violates the assumptions of type I regression (20). We therefore used type II regression to assess the quantitative effects of body size and temperature on substitution rates. However, before fitting type II regression models, we first determined whether body size and temperature had significant independent effects on substitution rates. This process was necessary because, for the data considered here, the largest animals all are endotherms, resulting in a positive correlation between body size and temperature. We therefore fitted type I multiple regression models for all of the data shown below. For the mitochondrial data that includes both ectotherms and endotherms, we fitted a model of the form $\ln(\alpha) = \beta \ln(M) - E(1/kT) + C$, and for the mammalian nuclear data, we fitted a model of the form $\ln(\alpha) = \beta \ln(M) + C$. This procedure simultaneously estimates the allometric scaling exponent, β, and activation energy, E, of substitution rates. Multiple regression analyses indicated significant independent effects for body size and temperature ($P < 0.05$) for all data except those for cytochrome *b* data shown in Figs. 1*C* and 2*C*. We note, however, that, on average, the type I regression coefficients were lower than the predicted values of -0.25 for β ($\bar{\beta} = -0.16$, $n = 6$) and 0.65 eV for E ($\bar{E} = 0.40$ eV, $n = 4$) (see *Appendix 4*).

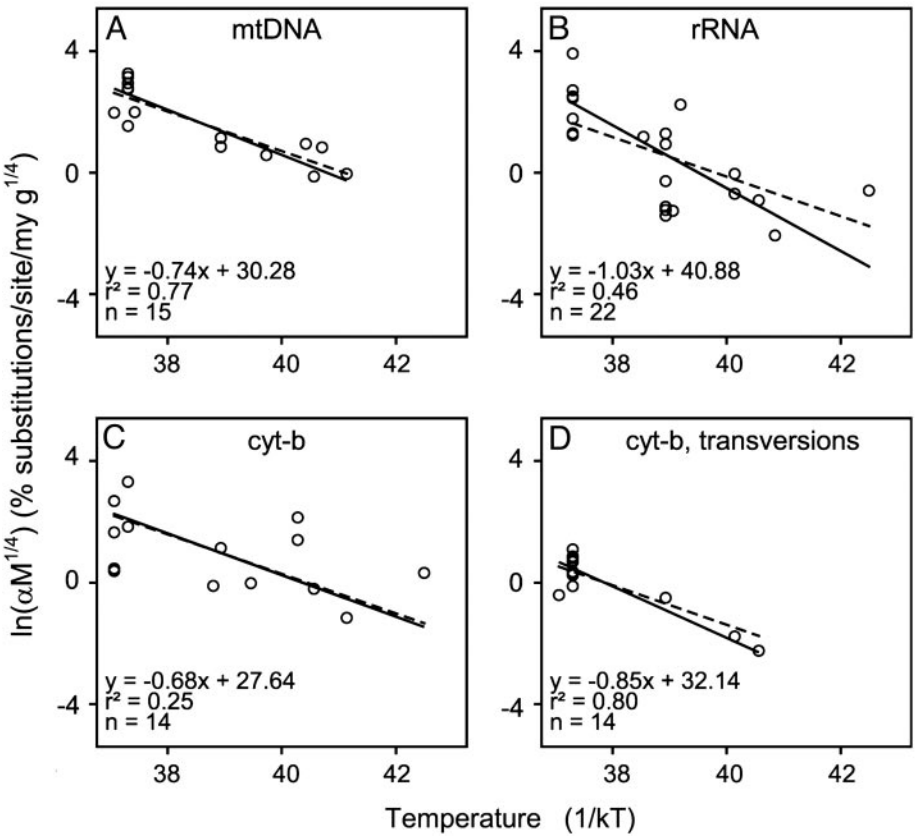

Fig. 1. Effect of temperature on nucleotide substitution rates after correcting for body mass by using Eq. **3**. Plots show four commonly used molecular clocks: the mitochondrial genome (mtDNA) (*A*), rRNA (12s and 16s combined) (*B*), all substitutions in the cytochrome *b* gene (*C*), and transversions in the cytochrome *b* gene (*D*). The solid lines were fitted by using type II linear regression; the dashed lines show the predicted slope of −0.65 eV. Data and sources are listed in *Appendix 2*.

Results and Discussion

Data support each of the model's three predictions. First, the logarithm of mass-corrected substitution rate is a linear function of inverse absolute temperature for the four molecular clocks from the mitochondrial genome (Fig. 1). Temperature accounts for 25–80% of the variation in mass-corrected substitution rates among diverse organisms, including endotherms (body temperatures of ≈35–40°C) and ectotherms from a broad range of thermal environments (≈0–30°C). The type II regression slopes of these lines all are close to the predicted value of −0.65 eV based on the kinetics of metabolism (Table 1). Thus, contrary to some recent reports (21), our results, which incorporated a wide range of body temperatures, indicate that nucleotide substitution rates are strongly temperature-dependent. Second, log-log plots of temperature-corrected substitution rates versus body mass all are well fitted by straight lines (r^2 = 0.23–0.74) for these four clocks, and the slopes all are close to the predicted value of −1/4 (Fig. 2 and Table 1). Substitution rates therefore show the same $M^{-1/4}$ allometric scaling as mass-specific metabolic rate B. Third, both endotherms and ectotherms (vertebrates and invertebrates) fall on the same lines in these relationships, supporting the prediction that $f\nu$ is approximately invariant across taxa for a given gene. Building on previous work showing correlations of substitution rate to body size (6), these results show that all animals cluster around a single line that is predicted by our model. Note that the model quantifies the combined effects of body size and temperature. Analyses that consider these variables separately, like much of the previous literature, explain much less of the observed variation in substitution rates (Table 2).

Still further support for the predicted mass dependence of molecular evolution (prediction 2) comes from analysis of two data sets on rates of silent substitutions in coding sequences of mammalian nuclear genomes. For globin data in primates, a log-log plot of substitution rate versus body mass gives a straight line with a slope close to the predicted value of −1/4 (−0.27, 95% confidence interval: −0.20 to −0.34; r^2 = 0.85, Fig. 3*A*). For a broader assortment of mammals and sequences (*Appendix 3*), a log-log plot also gives a straight line with a slope close to the predicted value of −1/4 (−0.21, 95% confidence interval: −0.18 to −0.23; r^2 = 0.77, Fig. 3*B*). And as predicted, both lines show very similar intercepts (24.79 and 24.81). Thus, it appears that mammalian nuclear genomes have slopes for the mass dependence of substitution rates that are similar to those observed in mitochondrial genomes for a broader range of taxa (Fig. 2), but intercepts which are slightly lower. We note, however, that in Figs. 1–3, observed values deviated by as much as 2.7-fold from the predicted values (Table 1). This residual variation likely indicates the importance of factors other than body size and temperature that affect measured substitution rates. Yet, these deviations of up to 2.7-fold are small compared with the ≈100-fold variation explained by our model.

The fact that the model predicts empirically observed substitution rates supports the hypothesis that there is a direct relationship between the rate of energy transformation in metabolism and the rate of nucleotide substitution. The number of substitutions per site per unit of mass-specific metabolic energy, $f\nu$, can be calculated from the y-intercepts (C) in Figs. 1–3: $f\nu = e^C/b_o$ (Eqs. **3** and **4**). Taking the fitted intercept of $C \approx 26$ for mtDNA (Table 1), and $b_o = 1.5 \times 10^8$ W·g$^{-3/4}$ (12), we obtain

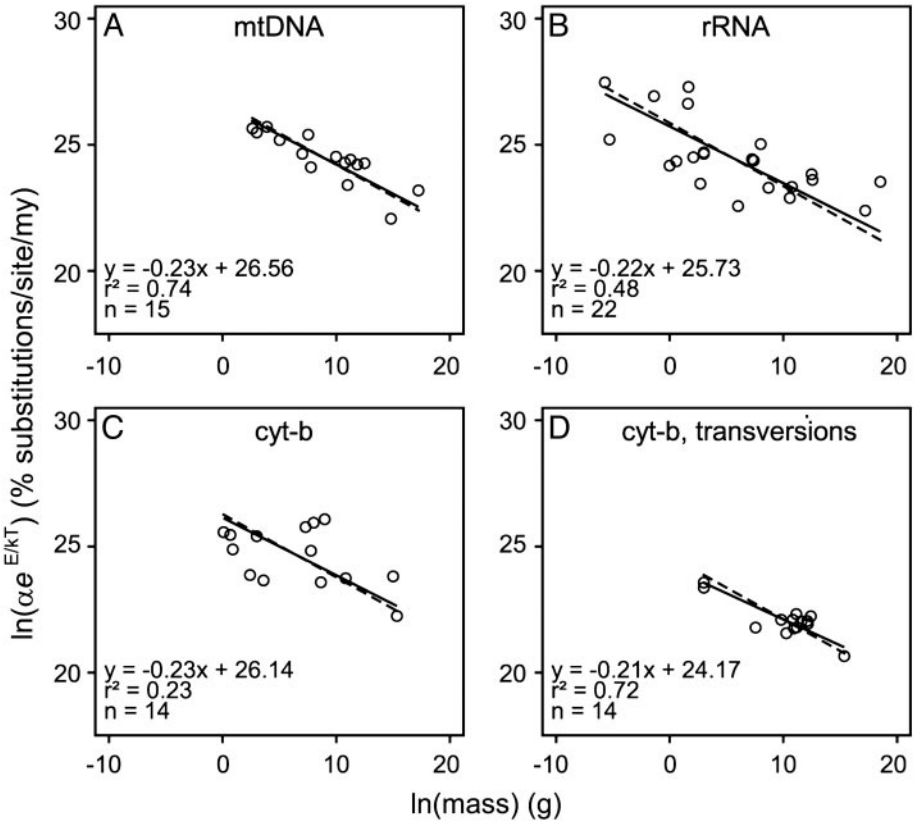

Fig. 2. Effect of body mass on nucleotide substitution rates after correcting for temperature by using Eq. **4**. Plots show the same data from the same four molecular clocks as in Fig. 1. The solid lines were fitted by using type II linear regression; the dashed lines show the predicted slope of −1/4. Data and sources are listed in *Appendix 2*.

$f\nu \approx 4 \times 10^{-13}$ g·substitutions·site^{-1}·J^{-1}. Thus, ≈2.4×10^{12} J of energy must be fluxed per g of tissue to induce one substitution per site in the mitochondrial genome.

Differences in the fitted intercepts, and therefore $f\nu$, among genes, genomes, and types of substitutions may reflect the influence of other factors in addition to body size and temperature. For example, f is known to vary from near 1 for synonymous codon sites and noncoding regions to near 0 for nonsynonymous sites, and ν differs between mitochondrial and nuclear genomes (19). The model could be fine-tuned to incorporate these and other possible sources of variation. In Table 1, the calculated intercepts for overall rates of substitution for mtDNA, rRNA, and cytochrome *b* are all ≈26. The intercept for cytochrome *b* transversions is lower (24.61), as are those for silent nuclear substitutions (24.79 and 24.81). These differences are consistent with current theory and data finding lower rates of transversions than transitions and lower overall rates of substitution in nuclear than in mitochondrial genomes (19).

We illustrate some of the evolutionary implications of this model with three examples. First, Fig. 4 shows estimates of a proposed molecular clock for mammalian divergence times (18), some of which differ substantially from fossil-based estimates. Molecular and fossil-based estimates are in close agreement for humans and chimpanzees (*Homo* and *Pan*, 5.5 My) because the clock calibrated in ref. 18 was disproportionately influenced by

Table 1. Parameter estimates and 95% confidence intervals (95% CI) for type II regression models depicted as solid lines in Figs. 1–3

	$\ln(\alpha M^{1/4})$ vs. $1/kT$		$\ln(\alpha e^{E/kT})$ vs. $\ln(M)$			
Gene/genome	Fitted slope (95% CI)	Predicted slope	Fitted slope (95% CI)	Predicted slope	Calculated intercept	Average residuals
mtDNA	−0.74 (−0.58, −0.90)	−0.65	−0.23 (−0.16, −0.31)	−0.25	26.71	1.6
rRNA	−1.03 (−0.66, −1.41)	−0.65	−0.22 (−0.15, −0.30)	−0.25	25.87	2.7
Cytochrome *b*	−0.68 (−0.42, −0.95)	−0.65	−0.23 (−0.16, −0.30)	−0.25	26.28	2.7
Cytochrome *b* transversions	−0.85 (−0.74, −0.95)	−0.65	−0.21 (−0.17, −0.24)	−0.25	24.61	1.4
Globin, primates			−0.27 (−0.20, −0.34)	−0.25	24.62	1.2
silent nuclear, various mammals			−0.21 (−0.18, −0.23)	−0.25	25.22	1.3
Average	−0.83	−0.65	−0.23	−0.25		1.8

The first four molecular clocks listed are from the mitochondrial genome, the last two are from the nuclear genome. Slopes and intercepts are calculated based on the predicted size and temperature dependence in Eq. **2** and are depicted as dashed lines in the figures. The average residual deviation for each gene or genome shown in Figs. 1–3 is listed in the final column. Average residuals were calculated by averaging the absolute deviations from the dashed lines in Figs. 1–3, and then converting these logarithmic averages to arithmetic values.

Table 2. A comparison of the correlations (r^2 values) of mitochondrial nucleotide substitution rates (α, % substitutions per site per My) versus temperature ($1/kT$) and the natural logarithm of body mass (g) without correction for body mass and temperature, and after correction by using Eqs. 3 and 4

	ln(α) vs. $1/kT$		ln(α) vs. ln(M)	
Gene/genome	Uncorrected	Mass corrected	Uncorrected	Temperature corrected
mtDNA	0.23	0.77	0.14	0.74
rRNA	0.03	0.46	0.13	0.48
Cytochrome *b*	0.13	0.25	0.09	0.23
Cytochrome *b* transversions	0.16	0.80	0.00	0.72

the preponderance of data for these and other similarly large mammals. However, their clock-estimated divergence date for Hystricognath rodents predates the fossil estimate by >2-fold (115 My vs. 56.5 My), and for the much smaller rodent genera *Mus* and *Rattus* by >3-fold (41 My vs. 12.5 My). Our model largely reconciles these discrepancies by incorporating the effects of body size and obtaining a date close to the fossil estimate (Fig. 4; we corrected only for mass, because these mammals have similar body temperatures). The procedure of taking the quarter-power average corrects for the greater influence of smaller taxa on rates of divergence because of their higher mass-specific metabolic rates (see *Appendix 4*).

Second, our model suggests how differences in body size might explain the "hominoid slowdown hypothesis," which proposed that rates of molecular evolution have slowed in hominoids since their split from Old World monkeys (22). Based on differences in average body mass between extant hominoids (50 kg) and Old World monkeys (7 kg), our model predicts a ≈0.6-fold slowdown [$=(7\text{ kg}/50\text{ kg})^{1/4}$], close to the estimated 0.7 (22).

Third, our model suggests that differences in temperature may account for the nearly 4-fold discrepancy between a molecular and a geological estimate of the age of notothenioid antarctic fishes (11 My vs. 38 My) (23). Assuming that the temperate-zone ectotherms used to calibrate the clock occurred at ≈15°C, whereas the notothenioid fishes occurred at ≈0°C, our model appears to reconcile this discrepancy ($e^{-E/k(273+15)}/e^{-E/k(273+0)} \approx 4$). These three examples illustrate how calibrating molecular clocks for body size and temperature may provide insights into evolutionary history. Metabolic rates of plants and microbes show similar body size and temperature dependence as animals

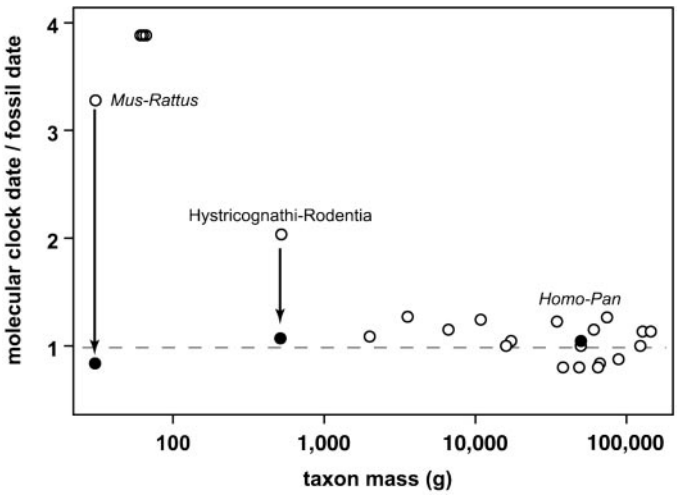

Fig. 4. Correcting for body size gives estimates of divergence dates that agree more closely with the fossil record (see *Appendix 3*). Open circles represent molecular clock estimates of divergence before accounting for effects of body size (18), and closed circles represent molecular clock estimates of divergence after accounting for effects of body size. Mass-corrected divergence dates were estimated by using the regression model in Fig. 3*B*. Arrows connect pairs of mass-corrected and uncorrected estimates, except for *Homo-Pan*, where these estimates are effectively indistinguishable. Correcting for mass has a much greater effect on clock-estimated divergences of small mammals, such as the rodent pair *Mus-Rattus*, because the uncorrected molecular clock in ref. 18 was calibrated mostly with large mammals. The horizontal, dashed line represents equality between molecular and fossil estimates.

(12). We expect that the theory developed here should be applicable to these organisms. This expectation is supported by a recent study showing the temperature dependence of mutation rates in plants (9).

These results also may have broader implications for understanding the factors controlling the overall rate of evolution. The central role of metabolic rate in controlling biological rate processes implies that metabolic processes also govern evolutionary rates at higher levels of biological organization where the neutral molecular theory does not apply. So, for example, the rate and direction of phenotypic evolution ultimately depends on the somewhat unpredictable action of natural selection. However, the overall rate of evolution ultimately is constrained by the turnover rate of individuals in

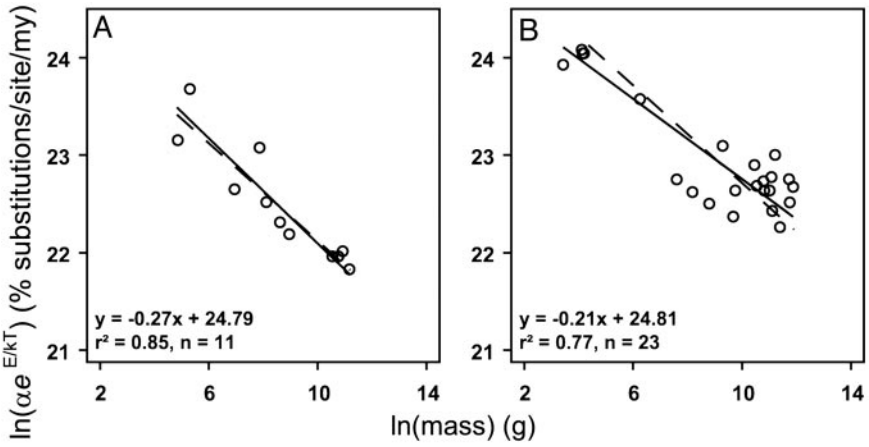

Fig. 3. Effect of body mass on silent rates of nucleotide substitution (% substitutions per site per My) in coding regions of the globin gene in primates (*A*) (6) and multiple coding regions of the nuclear genome for 23 pairs of mammalian lineages (*B*) (ref. 18 and *Appendix 3*).

populations, as reflected in generation time, and the genomic variation among individuals, as reflected in mutation rate (16, 24). Both of these rates are proportional to metabolic rate, so Eq. **1** also may predict the effects of body size and temperature on overall rates of genotypic and phenotypic change. Such predictions would be consistent with general macroevolutionary patterns showing that most higher taxonomic groups originate in the tropics where temperatures are high (25), speciation rates decrease with decreasing temperature from the equator to the poles (26, 27), biodiversity is highest in the tropics (28), and smaller organisms evolve faster and are more diverse than larger organisms (29).

We thank F. Allendorf, E. Charnov, H. Olff, V. Savage, T. Turner, and W. Woodruff for comments or discussions that improved this manuscript and S. Kumar for providing us with his data. J.F.G., G.B.W., and J.H.B. acknowledge support of the Thaw Charitable Trust and a Packard Interdisciplinary Science Grant. G.B.W., A.P.A., and J.H.B. were supported by the National Science Foundation. G.B.W. acknowledges the hospitality of the Mathematics Department at Imperial College, London, and the support of the Engineering and Physical Sciences Research Council.

1. Zuckerkandl, E. & Pauling, L. (1965) in *Evolving Genes and Proteins*, eds. Bryson, V. & Vogel, H. J. (Academic, New York), pp. 97–166.
2. Alroy, J. (1999) *Syst. Biol.* **48,** 107–118.
3. Smith, A. B. & Peterson, K. J. (2002) *Annu. Rev. Earth Planetary Sci.* **30,** 65–88.
4. Wray, G. A., Levinton, J. S. & Shapiro, L. H. (1996) *Science* **274,** 568–573.
5. Ayala, F. J., Rzhetsky, A. & Ayala, F. J. (1998) *Proc. Natl. Acad. Sci. USA* **95,** 606–611.
6. Martin, A. P. & Palumbi, S. R. (1993) *Proc. Natl. Acad. Sci. USA* **90,** 4087–4091.
7. Laird, C. D., McConaughty, B. L. & McCarthy, B. J. (1969) *Nature* **224,** 149–154.
8. Bleiweiss, R. (1998) *Proc. Natl. Acad. Sci. USA* **95,** 612–616.
9. Wright, S. D., Gray, R. D. & Gardner, R. C. (2003) *Evolution* **57,** 2893–2898.
10. Rand, D. M. (1994) *Trends Ecol. Evol.* **9,** 125–131.
11. Savage, V. M., Gillooly, J. F., Brown, J. H., West, G. B. & Charnov, E. L. (2004) *Am. Nat.* **163,** E429–E441.
12. Gillooly, J. F., Brown, J. H., West, G. B., Savage, V. M. & Charnov, E. L. (2001) *Science* **293,** 2248–2251.
13. Gillooly, J. F., Charnov, E. L., West, G. B., Savage, V. M. & Brown, J. H. (2002) *Nature* **417,** 70–73.
14. West, G. B., Brown, J. H. & Enquist, B. J. (1997) *Science* **276,** 122–126.
15. Kimura, M. (1968) *Nature* **217,** 624–626.
16. Fisher, R. A. (1930) *The Genetical Theory of Natural Selection* (Clarendon, Oxford).
17. Dobzhansky, T. (1951) *Genetics and the Origin of Species* (Columbia Univ. Press, New York).
18. Kumar, S. & Subramanian, S. (2002) *Proc. Natl. Acad. Sci. USA* **99,** 803–808.
19. Li, W. H. (1997) *Molecular Evolution* (Sinauer, Sunderland, MA).
20. Isobe, T., Feigelson, E. D., Akritas, M. G. & Babu, G. J. (1990) *Astrophys. J.* **364,** 104–113.
21. Bromham, L. & Penny, D. (2003) *Nat. Rev. Genet.* **4,** 216–224.
22. Seino, S., Bell, G. I. & Li, W. H. (1992) *Mol. Biol. Evol.* **9,** 193–203.
23. Eastman, J. T. & McCune, A. R. (2000) *J. Fish Biol.* **57,** 84–102.
24. Kimura, M. (1983) *The Neutral Theory of Molecular Evolution* (Cambridge Univ. Press, Cambridge, U.K.).
25. Jablonski, D. (1993) *Nature* **364,** 142–144.
26. Flessa, K. W. & Jablonski, D. (1996) in *Evolutionary Paleobiology*, eds. Jablonski, D., Erwin, D. H. & Lipps, J. H. (Univ. of Chicago Press, Chicago), pp. 376–397.
27. Stehli, F. G., Douglas, D. G. & Newell, N. D. (1969) *Science* **164,** 947–949.
28. Allen, A. P., Brown, J. H. & Gillooly, J. F. (2002) *Science* **297,** 1545–1548.
29. Brown, J. H., Marquet, P. A. & Taper, M. L. (1993) *Am. Nat.* **142,** 573–584.

Appendix 1. Relating Equation 2 to Kimura's Neutral Theory of Evolution

Here we show how Eq. 2 can be expressed in terms of generation time (G) so as to be consistent with Kimura's neutral theory. Kimura defined substitution rate as $a_G = fv_G$, where a_G is the nucleotide substitution rate/site/generation, f is the fraction of mutations that are selectively neutral, and v_G is the number of mutations/site/generation. In Eq. 2, we defined substitution rate based on physical time rather than generation time: $a = fvB$, where α is the substitutions/site/time, v is the number of mutations/site/Joule, and B is mass specific metabolic rate. Since generation time is inversely proportional to mass-specific metabolic rate, i.e., $G = g_0/B$ where g_0 is a constant, it therefore has the same mass and temperature dependence (1). We can therefore multiply both sides of our Eq. 2 by G to get Kimura's equation: $a_G = fv_G$, where $a_G = aG$ and $v_G = g_o v$.

1. Savage, V. M., Gillooly, J. F., Brown, J. H., West, G. B. & Charnov, E. L. (2004) *Am. Nat*. **163,** E429-E441.

Appendix 2. Data Analyzed in Figs. 1 and 2

Point	Locus	Group	Common name	Taxon 1	Taxon 2	α, %/my	Mass, g	T, °C
1	cytochrome *b*	Fish	Minnow	*Barbus spp.*		6.60E-1 (1)	1.46E+3 (2)	15 (2)
2	cytochrome *b*	Fish	Minnow	*Leuciscus peloponnensis*	*Telestes pleurobipunctatus*	9.00E-1 (3)	8.00E+3 (2)	15 (2)
3	cytochrome *b*	Reptile	Gecko	*Tarentola delalandii*		8.25E-1 (4)	1.98E+0 (5, 6)	21 (7)
4	cytochrome *b*	Invertebrate	Whelk	*Nucella lima*	*Nucella emerginata*	3.08E-1 (8)	1.09E+0 (8, 9)	9 (10)
5	cytochrome *b*	Reptile	Lizard	*Anolis oculatus*	*Anolis spp.*	7.15E-1 (11)	2.45E+0 (12)	26 (7)
6	cytochrome *b*	Mammal	Elephant	*Elephas maximus*	*Loxodonta africanus*	6.50E-1 (13)	3.26E+6 (14)	38 (15)
7	cytochrome *b*	Fish	Antarctic fish	Channichthyidae		1.86E-1 (16)	3.00E+3 (2)	0 (16)
8	cytochrome *b*	Reptile	Sea turtle	*Lepidochelys spp.*	*Caretta spp.*	2.08E-1 (17)	5.00E+4 (18)	25 (10)
9	cytochrome *b*	Mammal	Elephant/Mammoth	Elephantidae	Mammutidae	1.36E-1 (19)	4.58E+6 (14)	38 (15)
10	cytochrome *b*	Bird	Crane	Gruidae		6.00E-1 (20)	5.65E+3 (21)	40 (15)
11	cytochrome *b*	Amphibian	Newt	*Euproctus spp.*		3.83E-1 (22)	2.00E+1 (18)	13 (7)
12	cytochrome *b*	Bird	Goose	*Anser spp.*	*Brantus spp.*	2.10E+0 (23)	2.38E+3 (21)	40 (15)
13	cytochrome *b*	Bird	Honeycreeper	*Loxops virens*		8.00E-1 (24)	1.10E+1 (21)	40 (15)
14	cytochrome *b*	Bird	Tube-nosed sea bird	Oceanitinae		6.45E-1 (25)	3.68E+1 (21, 25)	40 (15)
15	mtDNA	Mammal	Mouse	*Mus musculus*	*Mus spretus*	3.78E+0 (18)	1.38E+1 (14)	37 (15)
16	mtDNA	Mammal	Dog	*Canis latrans*	*Canis lupus*	1.33E+0 (18)	2.16E+4 (14)	38 (15)
17	mtDNA	Mammal	Horse	*Equus spp.*		1.03E+0 (18)	2.67E+5 (14)	38 (15)
18	mtDNA	Mammal	Bear	*Ursus arctos*	*Ursus americanus*	9.75E-1 (18)	1.41E+5 (14)	38 (15)
19	mtDNA	Mammal	Primate	*Homo sapiens*	*Pan troglodytes*	1.05E+0 (18)	4.74E+4 (14)	38 (15)
20	mtDNA	Mammal	Whale	*Megaptera spp.*	*Baleanoptera spp.*	3.50E-1 (18)	3.04E+7 (14)	38 (15)
21	mtDNA	Bird	Goose	*Branta spp.*	*Anser spp.*	1.03E+0 (18)	2.38E+3 (21)	40 (15)
22	mtDNA	Reptile	Tortoise	*Gopherus spp.*	*Xerobates spp.*	3.08E-1 (18)	1.11E+3 (18)	19 (7)
23	mtDNA	Reptile	Sea turtle	*Chelonia mydas*		1.50E-1 (18)	5.90E+4 (18)	25 (10)
24	mtDNA	Amphibian	Newt	*Triturus crystatus*		4.18E-1 (18)	2.00E+1 (18)	13 (7)
25	mtDNA	Amphibian	Frog	*Rana spp.*		3.60E-1 (18)	5.00E+1 (18)	9 (7)
26	mtDNA	Fish	Shark	*Sphyrna spp.*	*Galeocerdo spp.*	1.55E-1 (18)	7.68E+4 (18)	14 (2)
27	mtDNA	Fish	Salmon	*Oncorynchus spp.*		3.50E-1 (18)	1.88E+3 (18)	12 (2)

28	mtDNA	Mammal	Whale	Mysticeti	Odontoceti	1.14E-1 (26)	2.73E+6 (14)	38 (15)
29	mtDNA	Invertebrate	Sea urchin	*Diadema antellarum*	*Diadema mexicanum*	8.97E-1 (27)	1.52E+2 (28)	25 (10)
30	rRNA	Fish	Antarctic fish	Notothenioidei		7.50E-2 (29)	3.00E+3 (2)	0 (16)
31	rRNA	Mammal	Gazelle	*Kobus ellipsiprymnus*	*Cephalophus maxwelli*	2.59E-1 (30)	3.91E+4 (14)	38 (15)
32	rRNA	Mammal	Horse	*Equus spp.*		6.61E-1 (31)	2.67E+5 (14)	38 (15)
33	rRNA	Invertebrate	Spider	*Aptostichus simus*		4.00E+0 (32)	3.33E-3 (32, 33)	16 (10)
34	rRNA	Fish	Cichlid fish	Cichlidae		1.46E-1 (34)	1.46E+1 (2)	24 (2)
35	rRNA	Amphibian	Newt	*Euproctus spp.*		1.90E-1 (22)	2.00E+1 (18)	13 (7)
36	rRNA	Amphibian	Newt	*Taricha spp.*	*Notophthalmus spp.*	2.35E-1 (22)	2.00E+1 (18)	16 (7)
37	rRNA	Mammal	Whale	Mysticeti	Odontoceti	1.56E-1 (35)	3.00E+7 (14)	38 (15)
38	rRNA	Mammal	Primate	*Homo sapiens*	*Pan troglodytes*	4.00E-1 (36)	4.74E+4 (14)	38 (15)
39	rRNA	Mammal	Seal	*Phoca vitulina*	*Halichoerus grypus*	3.90E-1 (36)	5.92E+3 (14)	38 (15)
40	rRNA	Mammal	Whale	*Balaenoptera musculus*	*Balaenoptera physalus*	4.90E-1 (36)	1.12E+8 (14)	38 (15)
41	rRNA	Mammal	Horse	*Equus caballus*	*Equus asinus*	5.30E-1 (36)	2.84E+5 (14)	38 (15)
42	rRNA	Fish	Subtropical fish	*Centropomus pectinatus*	*Centropomus medius*	4.17E-1 (37)	1.40E+3 (37)	25 (10)
43	rRNA	Invertebrate	Fiddler crab	*Sesarma spp.*		3.25E-1 (38)	9.92E-1 (39)	25 (10)
44	rRNA	Invertebrate	Fiddler crab	*Uca spp.*		4.50E-1 (40)	8.00E+0 (41)	25 (10)
45	rRNA	Reptile	Iguana	*Dipsosaurus spp.*	*Amblyrynchus spp.*	5.13E-1 (42)	1.61E+3 (43)	28 (7)
46	rRNA	Invertebrate	Cricket	*Laupala spp.*		5.10E+0 (24)	2.50E-1 (44)	25 (7)
47	rRNA	Invertebrate	Land snail	*Mandarina spp.*		6.19E+0 (45)	5.19E+0 (9, 46)	23 (2)
48	rRNA	Invertebrate	Copepod	*Euchaeta marina*	*Euchaeta rimana*	9.08E-1 (47)	5.00E-3 (48)	25 (10)
49	rRNA	Fish	Electric fish	Mormyriformes	Gymnotiformes	6.50E-2 (49)	4.07E+2 (2)	25 (2)
50	rRNA	Invertebrate	Isopod	Serolidae		3.70E-1 (50)	5.00E+0 (51)	0 (16)
51	rRNA	Invertebrate	Snail	*Littorina squalida*	*Littorina littorea*	1.10E-1 (52)	1.78E+0 (9)	11 (10)
52	cytochrome *b*-TV	Mammal	Goat/Sheep	*Capra spp.*	*Ovis spp.*	1.46E-1 (53)	6.85E+4 (14)	38 (15)
53	cytochrome *b*-TV	Mammal	Cow/Goat-Sheep	Bovinae	Caprinae	1.09E-1 (53)	1.07E+5 (14)	38 (15)
54	cytochrome *b*-TV	Mammal	Bovid/Giraffe-Deer	Bovidae	Giraffidae-Cervidae	8.65E-2 (53)	7.16E+4 (14)	38 (15)
55	cytochrome *b*-TV	Mammal	Ruminant/Camel	Ruminantia	Camelidae	8.28E-2 (53)	5.64E+4 (14)	38 (15)
56	cytochrome *b*-TV	Mammal	Ruminant/Pig	Ruminantia	Suidae	6.81E-2 (53)	2.88E+4 (14)	38 (15)
57	cytochrome *b*-TV	Mammal	Wildebeest	*Connochaetes taurinus*	*Connochaetes gnou*	1.10E-1 (54)	1.80E+5 (14)	38 (15)
58	cytochrome *b*-TV	Mammal	Cow/Nyala	*Bos spp.*	*Tragelaphus spp.*	1.33E-1 (54)	2.45E+5 (14)	38 (15)

59	cytochrome *b*-TV	Mammal	Gazelle	*Oreotragus spp.*	*Gazelle spp.*	1.17E-1 (54)	1.81E+4 (14)	38 (15)
60	cytochrome *b*-TV	Mammal	Cow/Sheep	*Bos spp.*	*Ovis spp.*	9.88E-2 (54)	1.89E+5 (14)	38 (15)
61	cytochrome *b*-TV	Mammal	Elephant/Mammoth	Mammutidae	Elephantidae	2.74E-2 (19)	4.65E+6 (14)	38 (15)
62	cytochrome *b*-TV	Bird	Booby and Gannet	*Morus spp.*	*Sula spp.*	1.00E-1 (55)	1.93E+3 (21)	40 (15)
63	cytochrome *b*-TV	Reptile	Sea turtle	*Lepidochelys spp.*	*Caretta spp.*	4.06E-2 (17)	5.00E+4 (18)	25 (10)
64	cytochrome *b*-TV	Amphibian	Newt	*Euproctus spp.*		5.00E-2 (22)	2.00E+1 (18)	13 (7)
65	cytochrome *b*-TV	Amphibian	Newt	*Taricha spp.*	*Notophthalmus spp.*	8.00E-2 (22)	2.00E+1 (18)	16 (7)

Divergence was estimated by direct sequencing for ribosomal RNA (rRNA, overall rates for 12s and 16s combined), cytochrome *b* (overall rate), and cytochrome *b* transversions. Overall rates of mitochondrial DNA evolution (mtDNA) were estimated using the restricted fragment length polymorphism method. Overall mass was calculated based on the quarter-power average (discussed in Appendix 4) for the taxa being compared.

1. Substitution rate calculated from divergence rate, p. 259 in (1), calibrated with fossil record. Body mass was calculated as the quarter-power average of 6 species in the genera *Barbus* and *Messinobarbus* with size data from (2). Average temperature was estimated based on the preferred habitat of these species from (2).

2. Substitution rate calculated from divergence rate, p. 230 in (3), calibrated with geological events. Body mass used was that reported for *Leuciscus peloponnensis* in (2). A mass estimate was unavailable for *Telestes pleurobipunctatus*. Temperature was estimated based on the preferred habitat of these species (2).

3. Substitution rate calculated from average divergence rate, p. 1217 in (4), calibrated with geological event. Body mass was calculated using the estimate for snout-vent length (40 mm) reported in (5) and the conversion formula for lizards in (6). Temperature based on mean annual temperature of the Canary Islands.

4. Substitution rate calculated from percent sequence divergence between *Nucella lima* and *Nucella emarginata*, p.2292 in (8), calibrated with fossil record, p. 2303 in (8). Body mass was calculated as the quarter power average of the two species using the average shells lengths reported for *Nucella lima* and *N. emerginata* (30 and 20 mm, respectively) in table 1 of (8), and the conversion

formula for whelks in (9). Temperature was estimated as the average of the sea surface temperatures for sites in the range of *Nucella* reported in table 1 of (8).

5. Substitution rate calculated from divergence rate, p. 254 in (11), calibrated with geological event. Body mass was calculated by quarter-power averaging mass estimates reported in (12) for all *Anolis spp.* Temperature was calculated as mean annual air temperature in the Lesser Antilles (7).

6. Substitution rate calculated from divergence rate, p. 1882 in (13), calibrated with fossil record. Body mass was calculated by quarter-power averaging mass estimates reported in (14) for the two species.

7. Substitution rate calculated from percent sequence divergence, p. 93, table 4 in (16), calibrated with geological event, p. 87 in (16). Body mass was calculated by quarter-power averaging body mass estimates reported in (2) for four species in the family Channichthyidae.

8. Substitution rate calculated from divergence rate, p. 5577 in (17), calibrated with fossil record. Body mass was taken to be the midpoint of the range of estimates reported by (18) for sea turtles. Temperature estimate based on average sea surface temperatures in tropical waters (10).

9. Substitution rate calculated from sequence divergence between Elephas and Mammut, p. 1192, table 1 in (19), calibrated with fossil record, p. 1190 in (19). Body mass was calculated by successively calculating quarter power averages of species, genera, and families using mass estimates from (14).

10. Substitution rate, p. 21 in (20), calibrated with fossil record. Body mass was calculated as the quarter-power average of species in the family Gruidae using data in (21).

11. Substitution rate, p. 140 in (22), calibrated with fossil record. Body mass estimate from (18). Temperature was calculated as the average of mean annual temperature estimates for the three *Euproctus* collection sites in France and Italy.

12. Substitution rate calculated from percent divergence rate (i.e., k value), p. 1403 in (23), calibrated with fossil record. Body mass was calculated by successively calculating quarter power averages of species and genera using mass estimates from (21).

13. Substitution rate from p. 539, figure 3 in (24), calibrated with geological event. Body mass estimated based on the mass of another species in the genus (*Loxops coccineus*).

14. Substitution rate for Oceanitinae, p.1366 in (25), calculated using K-2 corrected sequence divergence, and calibration point in fossil record. Body mass was estimated based on the quarter-power average of all taxa in the group Oceanitinae using mass data from (21).

15-27. RFLP-estimated rates of substitution were taken from table 2 in (18). Most rate estimates encompassed a range of values due to uncertainties associated with fossil-estimated divergence times. Where ranges were reported, we took the quarter-power average of the minimum and maximum values. For taxa where multiple rate estimates were reported using the same data (i.e., bears, tortoises, sea turtles), only one estimate was used to avoid problems of non-independence. Information on size and temperature estimates for these points follow.

15. Body mass was calculated as the quarter-power average of the two species using mass data from (14).

16. Body mass was calculated as the quarter-power average of the two species using mass data from (14).

17. Body mass was calculated as the quarter-power average of all species in the genus *Equus* using mass data from (14).

18. Body mass was calculated as the quarter-power average of the two species using mass data from (14).

19. Body mass was calculated as the quarter-power average of the two species using mass data from (14).

20. Body mass was calculated by successively calculating quarter power averages of species and then genera using mass data from (14).

21. Body mass was calculated by successively calculating quarter power averages of species and then genera using mass data from (21).

22. Body mass was calculated as the quarter-power average of the minimum and maximum values reported in (18). Temperature was calculated as the average of mean annual temperatures in the ranges of the two taxa using the database of (7).

23. Body mass was calculated as the quarter-power average of minimum and maximum values reported in (18). Temperature estimate based on average sea surface temperatures in tropical waters (10).

24. Body mass estimate from (18). Temperature based on mean annual temperature estimates of (7) throughout the species range.

25. Body mass estimate from (18). Temperature based on mean annual temperature estimates of (7) throughout the species range.

26. Body mass estimate from (18). Temperature estimate based on the species preferred habitat from (2).

27. Body mass estimate from (18). Temperature estimate based on the species preferred habitat from (2).

28. Substitution rate calculated from percent sequence divergence, p. 18 in (26), calibrated with fossil record. Mass was calculated by successively taking quarter power averages of species, genera, families, and finally the two suborders using data from (14).

29. Substitution rate calculated from divergence rate, p. 2376, table 2 in (27), calibrated with geological event. Mass estimate based on value reported for *Diadema setosum* in (28). Temperature based on sea surface temperatures at the Isthmus of Panama (10).

30. Substitution rate calculated from divergence rate, p. 861 in (29), calibrated with fossil record. Calculation based on the maximum genetic distance in table 2, using 38 MYA radiation of Notothenoids, and excluding species 1,18, 19, and 20 in the table, which the authors judged not to be part of the initial radiation.

31. Substitution rate calculated from percent divergence, p. 3973, table 1 in (30), calibrated with fossil record, p. 3976 in (30). Mass estimate based on the quarter-power average of the mass estimates for the two taxa using data from (14).

32. Substitution rate calculated from percent divergence, p. 346, table 2 in (31), calibrated with fossil record, p. 349, table 3 in (31). Body mass was calculated as the quarter-power average of all species in the genus *Equus* using mass data from (14).

33. Substitution rate, p. 906 in (32), calibrated with geological event. Body mass was calculated using the carapace length measurements reported by (32) and the length-weight conversion formula of. (33). Temperature calculated as mean annual temperature at sites where the species was collected using the database of (7).

34. Substitution rate calculated from divergence rate, p. 1094, table 1 in (34), calibrated with fossil record. Body mass was calculated using carapace length measurements reported by (32) and the length-weight conversion formula of (33). Average temperature was estimated based on the preferred habitat of these species from (2).

35. Substitution rate calculated from divergence rate, p. 140 in (22), calibrated with geological event. Mass estimate from (18). Temperature was calculated based on the average of mean annual temperature estimates for the three *Euproctus* collection sites in France and Italy.

36. Substitution rate calculated from divergence rate, p. 140 in (22), calibrated with geological event. Mass estimate from (18). Temperature was calculated based on the average of mean annual temperature estimates near the sampling location in Italy (7).

37. Substitution rate calculated from divergence rate, p. 945 in (35), calibrated with fossil record. Body mass was calculated by successively calculating quarter power averages of species, genera, families, and suborders using mass data from (14).

38-41. Substitution rate calculated as the average of the rates for 12s and 16s from table 2, p. 429 in (36), calibrated with fossil record and geological events. Body mass was calculated as the quarter-power average of the two species using mass data from (14).

42. Substitution rate calculated from percent divergence, p.199, table 3 in (37), calibrated with geological event, p. 204 in (37). Body mass was calculated as the quarter-power average of the two species using estimates in (37). Temperature based on sea surface temperatures at the Isthmus of Panama (10).

43. Substitution rate calculated from sequence divergence, p. 365 in (38), calibrated with geological event, p. 365 in (38). Body mass estimate used was that reported for *Sesarma curacaoense* in (39).

44. Substitution rate calculated from sequence divergence rate, p. 1065 in (40), calibrated with geological event. Body mass estimate used was a general value for *Uca* reported in (41).

45. Substitution rate calculated as the average of the rates for 12s and 16s on p. 427, table 2 in (42). Body mass is that of *Amblyrynchus cristatus* reported in (43). Temperature based on mean annual temperature estimate for the Galapagos Islands (7).

46. Substitution rate calculated from divergence rate, p. 541 in (24), calibrated with geological event. Body mass estimate from (44). Temperature estimate from average air temperature on Hawaii.

47. Substitution rate calculated from the average of the percent divergence for 12s and 16s, p. 464 in (45), calibrated with geological event, p. 460 in (45). Body mass calculated using the shell dimension estimates of (46) and a conversion formula for snails in (9).

48. Substitution rates calculated from divergence data, p. 86 in (47), assuming Isthmus of Panama closed 3 mya. Temperature based on sea surface temperatures at the Isthmus of Panama (10). Body mass estimated from that of *Euchaeta norvegica* reported in (48).

49. Substitution rate calculated from divergence rate, p. 1177 in (49), calibrated with fossil record. Body mass was calculated based on the quarter-power average of a subset of species for which body size estimates could be calculated in (2). Temperature based on preferred habitat description in (2).

50. Substitution rate, p. 499, table 1 in (50), calibrated with geological event. Mass is that of *Serolis pagenstecheri* in (51).

51. Substitution rate calculated as the average of the rates for 12s and 16s, p. 4 in (52), calibrated with fossil record. Mass estimate based on maximum size of *Littorina brevicula* reported in (9). Temperature calculated as average sea surface temperature (10).

52-56. Substitution rate estimates for transversions obtained from fig. 3 in (53). Mass estimates obtained by successively taking quarter power averages of species, genera, and families, and suborders within groups, and then quarter-power averaging across groups using mass data from (14).

57-60. Substitution rate estimates for transversions obtained from fig. 2 of (54). Mass estimates obtained by successively taking quarter power averages of species, genera, and families, and suborders within groups, and then quarter-power averaging across groups using mass data from (14).

61. Substitution rate calculated from the percent sequence differences between *Mammut* and *Loxodonta*, calibrated from the fossil record, p. 1192 in (19). Mass estimates obtained by successively taking quarter power averages of species, genera, and then families of mammals using mass data from (14).

62. Substitution rates calculated from percent sequence differences, p. 256 in (55), calibrated with the fossil record. Mass was calculated by successively taking quarter-power average of species and then genera using mass estimates from (21).

63. Substitution rates calculated from percent sequence differences, p. 5576, fig. 2 in (17), calibrated with the fossil record. Body mass was taken to be the midpoint of the range of estimates reported by (18) for sea turtles. Temperature estimate based on average sea surface temperatures in tropical waters (10).

64. Substitution rates calculated from divergence rate, p. 140 in (22), calibrated with the fossil record. Temperature was calculated based on the average of mean annual temperature estimates for the three *Euproctus* collection sites in France and Italy.

65. Substitution rates calculated from divergence rate, p. 140 in (22), calibrated with the fossil record. Temperature was calculated based on the mean annual temperature estimate for collection site in Italy.

1. Machordom, A. & Doadrio, I. (2001) Mol. Phylogenet. Evol. 18, 252- 263.

2. Froese, R. & Pauly, D., eds. (2004) FishBase, www.fishbase.org, (version 10/2004).

3. Zardoya, R. & Doadrio, I. (1999) *J. Mol. Evol.* **49,** 227-237.

4. Gubitz, T., Thorpe, R. S. & Malhotra, A. (2000) *Mol. Ecol.* **9,** 1213-1221.

5. Thorpe, R. S. (1991) *Syst. Zool.* **40,** 172-187.

6. Pough, F. H. (1980) *Am. Nat*. **115,** 92-112.

7. Legates, D. R. & Wilmott, C. J. (1990) *Theor. Appl. Climatol.* **41,** 11-21.

8. Collins, T. M., Frazer, K., Palmer, A. R., Vermeij, G. J. & Brown, W. M. (1996) *Evolution* **50,** 2287-2304.

9. Tokeshi, M., Ota, N. & Kawai, T. (2000) *J. Zool.* **251,** 31-38.

10. Casey, K. S. & Cornillon, P. (1999) *J. Climate* **12,** 1848-1863.

11. Malhotra, A. & Thorpe, R. S. (2000) *Evolution* **54,** 245-258.

12. Perry, G. & Garland, T. (2002) *Ecology* **83,** 1870-1885.

13. Fleischer, R. C., Perry, E. A., Muralidharan, K., Stevens, E. E. & Wemmer, C. M. (2001) *Evolution* **55,** 1882-1892.

14. Smith, F. A., Lyons, S. K., Ernest, S. K. M., Jones, K. E., Kaufman, D. M., Dayan, T., Marquet, P. A., Brown, J. H. & Haskell, J. P. (2003) *Ecology* **84,** 3403.

15. Prosser, C. L. (1973) *Comparative Animal Physiology* (Saunders, Philadelphia).

16. Eastman, J. T. & McCune, A. R. (2000) *J. Fish Biol.* **57,** 84-102.

17. Bowen, B. W., Nelson, W. S. & Avise, J. C. (1993) *Proc. Natl. Acad. Sci. USA* **90,** 5574-5577.

18. Martin, A. P. & Palumbi, S. R. (1993) *Proc. Natl. Acad. Sci. USA* **90,** 4087-4091.

19. Yang, H., Golenberg, E. M. & Shoshani, J. (1996) *Proc. Natl. Acad. Sci. USA* **93,** 1190-1194.

20. Krajewski, C. & King, D. G. (1996) *Mol. Biol. Evol.* **13,** 21-30.

21. Dunning, J. B. (1993) *CRC Handbook of Avian Body Masses* (CRC, Boca Raton, FL).

22. Caccone, A., Milinkovitch, M. C., Sbordoni, V. & Powell, J. R. (1997) *Syst. Biol.* **46,** 126-144.

23. Paxinos, E. E., James, H. F., Olson, S. L., Sorenson, M. D., Jackson, J. & Fleischer, R. C. (2002) *Proc. Natl. Acad. Sci. USA* **5,** 1399-1404.

24. Fleischer, R. C., McIntosh, C. E. & Tarr, C. L. (1998) *Mol. Ecol.* **7,** 533-545.

25. Nunn, G. B. & Stanley, S. E. (1998) *Mol. Biol. Evol.* **15,** 1360-1371.

26. Ohland, D. P., Harley, E. H. & Best, P. B. (1995) *Mol. Phylogenet. Evol.* **4,** 10-19.

27. Bermingham, E. & Lessios, H. A. (1993) *Proc. Natl. Acad. Sci. USA* **90,** 2734-2738.

28. Carreiro-Silva, M. & McClanahan, T. R. (2001) *J. Exp. Marine Biol. Ecol.* **262,** 133-153.

29. Bargelloni, L., Ritchie, P. A., Patarnello, T., Battaglia, B., Lambert, D. M. & Meyer, A. (1994) *Mol. Biol. Evol.* **11,** 854-863.

30. Allard, M. W., Miyamoto, M. M., Jarecki, L., Kraus, F. & Tennant, M. R. (1992) *Proc. Natl. Acad. Sci. USA* **89,** 3972-3976.

31. Oakenfull, E. A., Lim, H. N. & Ryder, O. A. (2000) *Conserv. Genet.* **1,** 341-355.

32. Bond, J. E., Hedin, M. C., Ramirez, M. G. & Opell, B. D. (2001) *Mol. Ecol.* **10,** 899-910.

33. Rogers, L. E., Hinds, W. T. & Buschbom, R. L. (1976) *Ann. Entomol. Soc. Am.* **69,** 387-389.

34. Vences, M., Freyhof, J., Sonnenberg, R., Kosuch, J. & Veith, M. (2001) *J. Biogeogr.* **28,** 1091-1099.

35. Milinkovitch, M. C., Meyer, A. & Powell, J. R. (1994) *Mol. Biol. Evol.* **11,** 939-948.

36. Pesole, G., Gissi, C., DeChirico, A. & Saccone, C. (1999) *J. Mol. Evol.* **48,** 427-434.

37. Tringali, M. D., Bert, T. M., Seyoum, S., Bermingham, E. & Bartolacci, D. (1999) *Mol. Phylogenet. Evol.* **13,** 193-207.

38. Schubart, C. D., Diesel, R. & Hedges, S. B. (1998) *Nature* **393,** 363-365.

39. Diesel, R., Schubart, C. D. & Schuh, M. (2000) *J. Zool.* **250,** 141-160.

40. Sturmbauer, C., Levinton, J. S. & Christy, J. (1996) *Proc. Natl. Acad. Sci. USA* **93,** 10855-10857.

41. Crane, J. (1975) *Fiddler Crabs of the World* (Princeton Univ. Press, Princeton).

42. Zamudio, K. R. & Greene, H. W. (1997) *Biol. J. Linnean Soc* .**62,** 421-442.

43. Nagy, K. A., Girard, I. A. & Brown, T. K. (1999) *Annu. Rev. Nutrit.* **19,** 247-277.

44. Otte, D. (1994) *The Crickets of Hawaii: Origin, Systematics and Evolution* (Orthopterists' Society, Philadelphia).

45. Chiba, S. (1999) *Evolution* **53,** 460-471.

46. Chiba, S. (1996) *Paleobiology* **22,** 177-188.

47. Braga, E., Zardoya, R., Meyer, A. & Yen, J. (1999) *Marine Biol.* **133,** 79-90.

48. Bamstedt, U. & Skjoldal, H. R. (1980) *Limnol. Oceanogr.* **25,** 304-316.

49. Alves-Gomes, J. A. (1999) *J. Exp. Biol.* **202,** 1167-1183.

50. Held, C. (2001) *Polar Biol.* **24,** 497-501.

51. Clarke, A. (1984) *Br. Antarctic Surv. Bull.***,** 37-53.

52. Hausdorf, B., Ropstorf, P. & Riedel, F. (2003) *Mol. Phylogenet. Evol.* **26,** 435-443.

53. Irwin, D. M., Kocher, T. D. & Wilson, A. C. (1991) *J. Mol. Evol.* **32,** 128-144.

54. Matthee, C. A. & Robinson, T. J. (1999) *Mol. Phylogenet. Evol.* **12,** 31-46.

55. Friesen, V. L. & Anderson, D. J. (1997) *Mol. Phylogenet. Evol.* **7,** 252-260.

Appendix 3. Method of analysis for data of Kumar and Subramanian (1)

Genetic divergence, *D*, among 23 pairs of mammalian taxa were computed based on synonymous substitutions in nuclear genomes (1). Clock-estimated dates of divergence were calculated by assuming a global clock for mammalian DNA evolution that was independent of body size (1). Fossil-estimated dates of divergence, t, obtained from (1) and other sources listed below, were used to calculate the substitution rate a (% substitutions/site/my; $a = 100 \times D/2t$). Masses were computed using the quarter-power averaging method described in Appendix 4. Because the 23 estimates of sequence divergence involved over 300 mammalian taxa (1), it was necessary to calculate quarter power averages on higher taxonomic groups. If the pair of species used to calculate a substitution rate belonged to the same genus, the quarter power average, M_q, was calculated based on the masses of the two extant species. If the two species belonged to different genera, but the same family, M_q was first calculated separately for each genus based on the masses of all species in the genus, and then again across the two genera. A similar, hierarchical approach was used to calculate values of M_q for pairs of species that varied at higher taxonomic levels (subfamily, family, suborder). Quarter-power averages were calculated using an extensive database on extant and extinct mammals (2). We specifically excluded from analysis data on divergences of orders and superordinal groups because the quarter-power averaging method assumes that extant taxa are similar in size to their ancestors, and because the radiation of mammalian orders near the K-T boundary (~65 My) involved pronounced and rapid changes in the body sizes of many lineage (3). Results in Figs. 3-4 are qualitatively identical if these data on deeper divergences are included.

Appendix 3. Continued.

Taxon 1	Taxon 2	Mass 1, g	Mass 2, g	Avg. Mass, g	*D*	Clock date, my	Fossil date, my	Substitution rate, %/site/my
Rodentia	Hystricognathi	5.23E+02	5.18E+02	5.20E+02	0.578	115 (1)	56.5 (4)	0.51
Cetacea	Ruminantia	1.10E+06	3.18E+04	1.28E+05	0.188	60 (1)	53 (1)	0.18
Cetacea	Suina	1.10E+06	3.78E+04	1.44E+05	0.220	60 (1)	53 (1)	0.21
Ruminantia	Tylopoda	3.18E+04	2.18E+05	7.41E+04	0.306	67 (1)	53 (1)	0.29
Ruminantia	Suina	3.18E+04	3.78E+04	3.46E+04	0.276	65 (1)	53 (1)	0.26
Canidae	Felidae	8.74E+03	1.37E+04	1.09E+04	0.234	46 (1)	37 (1)	0.32
Catarrhini	Platyrrhini	8.78E+03	1.71E+03	3.56E+03	0.146	47 (1)	37 (1)	0.20
Bovinae	Caprinae	2.64E+05	6.51E+04	1.23E+05	0.090	20 (1)	20 (1)	0.23
Bovoidea	Cervoidea	5.89E+04	6.27E+04	6.07E+04	0.080	23 (1)	20 (1)	0.20
Cercopithecidae	Hominidae	7.06E+03	5.43E+04	1.72E+04	0.088	23 (1)	22 (5)	0.20
Cercopithecidae	Hylobatidae	7.06E+03	6.24E+03	6.63E+03	0.070	23 (1)	20 (1)	0.18
Hominidae	Hylobatidae	5.43E+04	6.24E+03	1.59E+04	0.046	15 (1)	15 (6)	0.15
Homo spp.	*Pan spp.*	6.50E+04	3.89E+04	4.99E+04	0.022	5.5 (1)	5.5 (1)	0.20
Catarrhini	Strepsirhini	8.78E+03	6.80E+02	2.00E+03	0.260	63 (1)	58 (5)	0.22
Gerbillinae	Cricetinae	5.83E+01	6.88E+01	6.33E+01	0.278	66 (1)	17 (7)	0.82
Gerbillinae	Murinae	5.83E+01	6.38E+01	6.09E+01	0.288	66 (1)	17 (7)	0.85
Murinae	Cricetinae	6.38E+01	6.88E+01	6.62E+01	0.278	66 (1)	17 (7)	0.82
Mus spp.	*Rattus spp.*	1.03E+01	1.38E+02	3.07E+01	0.182	41 (1)	12.5 (8)	0.73
Homo spp.	*Gorilla spp.*	6.50E+04	1.24E+05	8.86E+04	0.022	7 (1)	8 (6)	0.14
Homo spp.	*Pongo spp.*	6.50E+04	3.70E+04	4.86E+04	0.044	8 (1)	10 (9)	0.22
Pan spp.	*Gorilla spp.*	3.89E+04	1.24E+05	6.66E+04	0.026	6.7 (1)	8 (6)	0.16
Pan spp.	*Pongo spp.*	3.89E+04	3.70E+04	3.79E+04	0.042	8 (1)	10 (9)	0.21
Gorilla spp.	*Pongo spp.*	1.24E+05	3.70E+04	6.47E+04	0.046	8 (1)	10 (9)	0.23

1. Kumar, S. & Subramanian, S. (2002) *Proc. Natl. Acad. Sci. USA* **99,** 803-808.

2. Smith, F. A., Lyons, S. K., Ernest, S. K. M., Jones, K. E., Kaufman, D. M., Dayan, T., Marquet, P. A., Brown, J. H. & Haskell, J. P. (2003) *Ecology* **84,** 3403-3403.

3. Alroy, J. (1998) *Science* **280,** 731-734.

4. Foote, M., Hunter, J. P., Janis, C. M. & Sepkoski, J. J. (1999) *Science* **283,** 1310-1314.

5. Goodman, M., Porter, C. A., Czelusniak, J., Page, S. L., Schneider, H., Shoshani, J., Gunnell, G. & Groves, C. P. (1998) *Mol. Phylogenet. Evol.* **9,** 585-598.

6. Nowak, M. A. (1997) *Walker's Mammals of the World* (Johns Hopkins Univ. Press, Baltimore).

7. Robinson, M., Catzeflis, F., Briolay, J. & Mouchiroud, D. (1997) *Mol. Phylogenet. Evol.* **8,** 423-434.

8. Jaeger, J. J., Tong, H. & Denys, C. (1986) *C. R. Acad. Sc. Paris* **302,** 917-922.

9. Andrews, P. & Cronin, J. (1982) *Nature* **297,** 541-546.

Appendix 4. "Quarter-Power Averaging" method for body masses of descendent lineages

Our model predicts that the nucleotide substitution rate, a, at a given moment in time will vary with body size and temperature as:

$$a = fvB = fvb_o M^{-1/4} e^{-E/kT} \qquad [2]$$

Equation 2 implies that the substitute rates of two descendent lineages, $a_1(t)$ and $a_2(t)$, will vary through time as a consequence of evolutionary changes in mass and/or temperature. The number of nucleotide substitutions per site that will accrue for the two descendent lineages by time t, $N_1(t)$ and $N_2(t)$, is calculated by integrating over the time interval, i.e., $N_1(t) = \int_0^t a_1(t)dt$ and $N_2(t) = \int_0^t a_2(t)dt$. If temperature remains fixed ($B_o = b_o e^{-E/kT}$), the sequence divergence, $D(t)$ between the two lineages since they diverged from a common ancestor is therefore:

$$D(t) = N_1(t) + N_2(t) = \int_0^t (a_1(t) + a_2(t))dt = fvB_o \int_0^t (M_1(t)^{-1/4} + M_2(t)^{-1/4})dt \qquad [4.1]$$

where $M_1(t)$ and $M_2(t)$ are the masses of the two descendent lineages at some time t since diverging from their common ancestor at $t = 0$, $M_1(0)=M_2(0)$ is the body mass of that common ancestor, and $M_1(t)$ and $M_2(t)$ are the body sizes of the two extant taxa at time t.

Most analyses assume that the substitution rates of the two descendant lineages are equal and remain constant through time (i.e., $a_1(t) = a_2(t) = a$). In this case, Eq. 4.1 reduces to $D(t) = D = 2at$, yielding the formula for substitution rate used in this paper: $a = D/2t$. Generally, though, the substitution rate will vary between the two descendent lineages, but it is not possible to integrate Eq. 4.1 without knowing how the masses change with time. However, if the change in mass is slow then

$$D(t) \approx fvB_o(M_1^{-1/4}(t) + M_2^{-1/4}(t))t = 2fvBM_q^{-1/4}t \qquad [4.2]$$

Here $M_q^{-1/4}$ is the "quarter power average" of the two descendent lineages, defined as $M_q = \left((M_1(t)^{-1/4} + M_2(t)^{-1/4})/2\right)^{-4}$. This approximation is valid provided that $d\ln M_{1,2}/d\ln t << 8$, or, equivalently, $d\ln a/d\ln t << 2$. This follows from expanding Eq. 4.1 in a Taylor series expansion in powers of t.

For all analyses presented in this paper, body mass effects within and across lineages were estimated based on the "quarter-power average" of mass, which is somewhat lower in magnitude than the geometric mean, but much lower than the arithmetic mean. Note that Eq. 4.1, and consequently the quarter power averaging method, implies that smaller bodied taxa have a disproportionately large influence on sequence divergence and thus on the calculated substitution rate between two descendent lineages. It also shows that problems may arise in attempting to estimate divergence dates in deep evolutionary time if ancestors of the extant taxa of interest are very different in size, and/or occur in very different thermal environments in the case of ectotherms.

Without knowing how mass evolves with time, it is not possible to estimate corrections for the approximation expressed in Eq. 4.2. We therefore used Type II linear regression to account for errors in the mass and temperature estimates (the two predictor variables of substitution rate) that are introduced by using the approximations for mass and temperature discussed above.